NONLINEAR AXISYMMETRIC AND THREE-DIMENSIONAL VORTICITY DYNAMICS IN A SWIRLING JET MODEL*

J.E. MARTIN
Department of Mathematics
Christopher Newport University
Newport News, VA 23606-2998

E. MEIBURG
Department of Aerospace Engineering
University of Southern California
Los Angeles, CA 90089-1191

Abstract

The mechanisms of vorticity concentration, reorientation, and stretching are investigated in a simplified swirling jet model, consisting of a line vortex along the jet axis surrounded by a jet shear layer with both azimuthal and streamwise vorticity. Inviscid three-dimensional vortex dynamics simulations demonstrate the nonlinear interaction and competition between a centrifugal instability and Kelvin-Helmholtz instabilities feeding on both components of the base flow vorticity. Under axisymmetric flow conditions, it is found that the swirl leads to the emergence of counterrotating vortex rings, whose circulation, in the absence of viscosity, can grow without bounds. Scaling laws are provided for the growth of these rings, which trigger a pinch-off mechanism resulting in a strong decrease of the local jet diameter. In the presence of an azimuthal disturbance, the nonlinear evolution of the flow depends strongly on the initial ratio of the azimuthal and axisymmetric perturbation amplitudes. The long term dynamics of the jet can be dominated by counterrotating vortex rings connected by braid vortices, by like-signed rings and streamwise braid vortices, or by wavy streamwise vortices alone.

*Support by the National Science Foundation under grant CTS-9196004 to EM, and through matching funds provided by the Electric Power Research Institute, is gratefully acknowledged. JEM was supported by the National Aeronautics and Space Administration under NASA Contract No. NAS1-19480 while in residence at the Institute for Computer Applications in Science and Engineering (ICASE), NASA Langley Research Center, Hampton, VA 23681-0001. Computing resources were provided by the NSF-supported San Diego Supercomputer Center.

1 Introduction

Swirling jets represent one of a handful of paradigm flows that, while of great practical significance, allow for the fundamental study of complex but generic dynamical processes and their interactions. They feature prominently in a variety of applications in such fields as propulsion, combustion, and mixing. At the same time, atmospheric conditions can give rise to swirling flows in nature, with both wake and jet-like axial velocity profiles. Examples concern tornados, dust devils and water spouts. All of the above situations are characterized by a complex interplay of a variety of competing dynamical mechanisms. The axial velocity profiles typically allow for shear induced instabilities similar to those encountered in nonswirling flows. However, the additional presence of swirl can result in an unstable radial stratification, thereby leading to centrifugal instabilities as well. Furthermore, the swirl can give rise to standing or propagating nonlinear inertial waves, similar to the internal waves observed in flows with density stratification. Finally, under certain conditions swirling jets are known to produce vortex breakdown events, an important generic phenomenon for which a universally accepted explanation is still elusive. An improved understanding of these mechanisms and their mutual coupling is a prerequisite for the successful development of active and passive control strategies employing sound, nozzle geometry and motion, or micromachines, with the goal of tailoring the flow such as to generate the desired operating conditions.

An introduction into the basic physics of swirling flows is given by Gupta et al.[1], while some more advanced aspects pertaining mostly to confined flows are reviewed by Escudier.[2] Early analytical investigations were mostly directed at finding similarity solutions to simplified equations and boundary conditions,[3] and at determining the linear stability of various combinations of axial velocity profiles and swirl.[4,5,6,7,8] Experimental investigations of swirling jets for the most part have addressed the issue of mean flow profiles and averaged turbulent transport properties.[9,10,11,12] Only recently have researchers begun to pay attention to the dominant role played by the underlying vortical flow structures and their dynamical evolution, e.g. Panda and McLaughlin.[13] These authors point out the crucial role played by axisymmetric and helical instability waves, emphasizing the importance of a *structure-based* understanding of the flow dynamics.

To our knowledge, no axisymmetric or three-dimensional nonlinear computations aimed at elucidating the fundamental dynamics of swirling jets are reported in the literature. However, the recent axisymmetric computational results obtained by Lopez,[14] Brown and Lopez,[15] and Lopez and Perry[16] for an internal swirling flow, and by Krause and colleagues for the vortex breakdown phenomenon (reviewed by Althaus et al.[17]) suggest that such computations can provide some fundamental insight into the flow physics of swirling jets.

For the purpose of studying the nonlinear dynamical interaction of shear and centrifugal instabilities in swirling jets, we recently introduced a simplified model[18] that is an extension to earlier ones proposed by Batchelor and Gill,[19] Rotunno,[20] and Caflisch, Li and Shelley.[21] It lends itself well to analytical linear stability calculations, as well as to nonlinear Lagrangian vortex dynamics simulations. The model consists of an axial centerline vortex,

which is surrounded by a nominally axisymmetric vortex sheet containing both streamwise and circumferential vorticity. While this model has obvious limitations when it comes to reproducing the detailed features of experimentally generated, and often geometry dependent velocity profiles, its simplicity offers several advantages. First of all, it allows for some analytical progress[18] in terms of a straightforward linear stability analysis, which illuminates the competition of centrifugal and Kelvin-Helmholtz instability waves. In particular, the results show that centrifugally stable flows can become destabilized by sufficiently short Kelvin-Helmholtz waves. Secondly, the model enables us to study the nonlinear interaction and competition of the various instability mechanisms involved, by means of fully nonlinear numerical calculations.

Some preliminary nonlinear simulations for axisymmetric perturbations were reported by Martin and Meiburg,[22] who showed that, under certain circumstances, *counterrotating* vortex rings emerge in the braid regions between the primary vortex rings generated by the Kelvin-Helmholtz instability of the axisymmetric shear layer. These counterrotating vortex rings can trigger a dramatic decrease in the local jet diameter. A further interesting observation shows the circulation of the swirling vortex rings to be time-dependent, in contrast to the vortex rings found in nonswirling jets. The dynamics of these swirling vortex rings represents an interesting research area in its own right. While nonswirling rings have been the subject of considerable theoretical, experimental, and computational research (Shariff and Leonard,[23] and references therein), much less is known about vortex rings with swirl, in part because of the considerable difficulties one encounters when trying to generate them experimentally. On the other hand, several recent theoretical investigations addressing the form and stability of isolated swirling vortex rings[24,25,26,27] can be expected to stimulate further efforts in this direction.

After a brief discussion of the flow model in section 2, we will investigate the nonlinear axisymmetric evolution of the above swirling jet model in more detail in section 3. In particular, the formation of recirculation regions will be analyzed in detail, and scaling laws for the time-dependent growth of the vortex ring circulations will be derived. In section 4, we will extend the numerical investigation to fully three-dimensionally evolving swirling jets, by imposing azimuthal perturbations in addition to the axisymmetric ones. The azimuthal perturbations can trigger additional instabilities of the rings or the braid regions. The simulations to be discussed will then allow us to investigate the nonlinear interplay of the competing instabilities for various values of the governing dimensionless parameters.

2 Flow Model and Numerical Technique

The present flow model of an axial line vortex surrounded by a nominally axisymmetric cylindrical shear layer containing streamwise and circumferential vorticity represents an extension of earlier ones investigated by several researchers, dating back to the analyses by Batchelor and Gill[19] as well as Rotunno[20] of the stability of an axisymmetric layer of circular or helical vortex lines. More recently, Caflisch, Li and Shelley[21] introduced the effect of swirl by placing the additional line vortex at the center of the axisymmetric layer.

However, their unperturbed vortex sheet had an axial vorticity component only, so that a jet-like velocity component was absent. In the present investigation, we employ a slightly more complicated model (Fig. 1), consisting of a line vortex of strength Γ_c at radius r=0, surrounded by a cylindrical vortex sheet at $r = R$. The unperturbed axisymmetric vortex sheet contains both azimuthal vorticity (corresponding to a jump ΔU_x in the axial velocity) and streamwise vorticity (representing a jump ΔU_θ in the circumferential velocity). The strength of the vortex sheet is taken to be equal and opposite to that of the line vortex. The vortex lines in the sheet hence are of helical shape, with their pitch angle ψ being

$$\psi = \tan^{-1}\left(\frac{\Delta U_\theta}{\Delta U_x}\right) \tag{1}$$

These particular features of our model were chosen on the basis of the following considerations. While an axisymmetric cylindrical layer of *circular* vortex lines represents a unidirectional flow with a top hat like profile shape, *helical* vortex lines result in an additional azimuthal velocity component, which jumps at the location of the vortex layer. If there is no streamwise circulation present at radii smaller than that of the cylindrical layer, this azimuthal velocity component vanishes inside the cylinder and exhibits a $1/r$-dependence on the outside. Consequently, since the magnitude of the circulation increases across the vortical layer, this flow is centrifugally stable on the basis of Rayleigh's circulation theorem. However, if some streamwise circulation is contained inside the cylinder, and if this circulation is of opposite sign to the streamwise circulation of the layer itself, then the magnitude of the circulation can decrease across the vortical layer, so that we obtain a centrifugally unstable flow. The line vortex at the center of the jet is introduced exactly for this purpose. Its strength is taken to be equal and opposite to that of the streamwise circulation contained in the vortical layer, in order that the azimuthal velocity component of the base flow vanishes outside the jet. In this way, our simplified model mimicks a swirling jet entering fluid at rest. The fluid velocity profile associated with our model is sketched in Fig. 1 as well.

By introducing both axial and azimuthal vorticity along with the central line vortex, this model allows for the investigation of competing Kelvin-Helmholtz and centrifugal instabilities, which can be expected to lead to interesting nonlinear dynamical behavior. For the nonswirling top hat jet velocity profile it is known that axisymmetric and helical perturbations will result in the formation of vortex rings or helices, respectively, all of the same sign.[28,29] For purely swirling flow, on the other hand, Caflisch et al.[21] demonstrated that axisymmetric perturbations lead to the emergence of counterrotating vortex rings. By superimposing a top hat streamwise velocity profile upon the purely swirling flow, we hence expect a breaking of the symmetry exhibited by the purely swirling flow alone. Conversely, introducing swirl into the nonswirling jet flow should lead to a tendency to form azimuthal vorticity of a sign opposite to that of the vortex rings which evolve as a result of the pure Kelvin-Helmholtz instability. Additional azimuthal disturbances will render the flow field fully three-dimensional. Both the swirling vortex rings as well as the braid regions connecting them may develop instabilities that can lead to the formation of concentrated streamwise vorticity.

In order to compute the nonlinear evolution of the flow in response to certain imposed perturbations, we employ a vortex filament technique that is essentially identical to the one used in earlier investigations of plane shear layers, wakes, and jets.[22,28,29,30,31,32] It is based on the theorems of Kelvin and Helmholtz and follows the general concepts reviewed by Leonard[33] and Meiburg.[34] A detailed account of the technique is provided in these earlier references.

For the numerical simulations of the simple jet model, we limit ourselves to the temporally growing problem, in spite of the spatial growth exhibited by a typical experimental flow field. We face a trade-off here, as the spatially growing simulation would require that we extend the control domain over several streamwise wavelengths, so that the numerical resolution per streamwise wavelength would necessarily suffer. In addition, the streamwise boundary conditions pose a much more severe problem in spatially growing flows. In the present investigation we opt for the temporally growing approach. Previous experience concerning the simulation of nonswirling and swirling jets justifies this approach, as it demonstrates that centrifugal and shear instabilities represent the dominant mechanisms in the evolution of the jet. These mechanisms are captured by the temporally growing flow, so that we can expect to gain significant insight into the dynamical evolution of these flows on the basis of the temporal growth approach. Under this assumption, we can concentrate the numerical resolution on one streamwise wavelength, which allows us to take the calculation farther in time.

The wavelength in the axial direction, i.e., the length of the control volume, is based on Michalke and Hermann's[35] stability analysis for the spatially evolving nonswirling jet. By using Gaster's[36] transformation, we obtain the wavelength of maximum growth for the temporally evolving flow as approximately 2π. One cannot necessarily expect the linearly most unstable wavelength to dominate the nonlinear regime as well. However, as our interest lies in simulating the evolution of a slightly perturbed flow from the linear regime all the way into the nonlinear one, starting with the linearly most unstable wavelength represents the obvious approach. Whether or not this wavelength continues to dominate the nonlinear regime, or if it changes due to pairing or other nonlinear interaction mechanisms, can only be determined by extending the simulation farther into the nonlinear regime, under explicitly imposed perturbations or random roundoff errors. We do not investigate this issue in the present study.

One streamwise wavelength is typically discretized into 105 filaments. Each filament initially contains 123 segments in the circumferential direction. These numbers emerged from test calculations, in which we refined the discretization until a further increase in resolution resulted in very small changes. The Biot-Savart integration is carried out with second order accuracy both in space and in time by employing the predictor-corrector time-stepping scheme, in conjunction with the trapezoidal rule for the spatial integration. As the flow structure develops nonlinearly, the vortex filaments undergo considerable stretching. To maintain an adequate resolution, the cubic spline representation of the filaments is used to introduce additional nodes, based on a criterion involving distance and curvature.[30] Furthermore, the time-step is repeatedly reduced as local acceleration effects increase. The

filament core radius σ decreases as its arclength increases, to conserve its total volume. In order to assess the accuracy and convergence of the vortex filament simulations, we presented in Martin and Meiburg[28] a comparison of the numerical and analytical growth rates for the axial Kelvin-Helmholtz instability of the *nonswirling* jet. This comparison showed that the simulation overpredicts the growth rate, which is due to the fact that the filaments do not deform from a circular cross section under strain. In Figure 2, a comparison is shown for the growth rates of a *purely swirling* flow. It can be seen that the numerical growth rate reproduces the exact one to a high degree of accuracy.

We take the streamwise velocity difference between the centerline and infinity as the characteristic velocity. The thickness of the axisymmetric shear layer serves as the characteristic length scale, which results in the filament core radius $\sigma = 0.5$. The nominal jet radius R is taken to be 5, and we obtain the ratio of jet radius R and momentum thickness θ of the jet shear layer as $R/\theta = 22.6$. Hence, the ratio $R/\sigma \gg 1$, and we are well within the range of validity of the filament model.

3 Results

3.1 Axisymmetric Case

As a first step, we discuss the nonlinear evolution of a strictly axisymmetric configuration, for which some preliminary results were reported by Martin and Meiburg.[22] The swirling jet is centrifugally unstable under Rayleigh's circulation theorem, allowing us to investigate the competition between the Kelvin-Helmholtz instability of the azimuthal vorticity component and the centrifugal instability feeding on the streamwise vorticity.

The initial axisymmetric perturbation displaces the vortex filament centerlines in the radial direction, with an amplitude, ϵ_1, of five per cent of the nominal jet radius. A filament's perturbed radius r' is then determined by the equation

$$r' = r\left(1 - \epsilon_1 \sin\left(2\pi x/\lambda\right)\right) \tag{2}$$

in which λ is the streamwise wavelength, and r is the distance of the filament centerline from the jet axis. A typical development of the flow field is shown in Figure 3 for the relatively large velocity ratio of $\Delta U_\theta/\Delta U_x = 8.2$. This parameter value indicates that the jump in the azimuthal velocity component across the jet shear layer is much larger than that of the axial component, so that, for the unperturbed flow, the vortex lines are predominantly oriented in the streamwise direction. Figure 3a (time=0.039) shows a side view, i.e., those filament sections located at $y > 0$, of an early configuration of the vortex filaments, along with contours of the azimuthal vorticity component (Fig. 3b). For clarity, two streamwise wavelengths are shown. Both graphs indicate that the azimuthal vorticity component points in the same direction everywhere in the vortex sheet, in a fashion similar to the axisymmetric Kelvin-Helmholtz instability of nonswirling jets. The contour plot reflects the early stages of ring formation due to the Kelvin-Helmholtz instability of the azimuthal vorticity component. By time 0.801 (Fig. 4a), on the other hand, a new phenomenon can be observed, namely

the reorientation of certain vortex filament segments in the opposite azimuthal direction. Near $x = \pi$ and $x = 3\pi$, the rings that were already emerging at $t = 0.039$ continue to grow. Their vorticity is of the same sign as that in a corresponding nonswirling jet. At $x = 0$ and $x = 2\pi$, however, the vortex filaments reverse their direction, which causes them to form regions of azimuthal vorticity of opposite sign. This reflects the influence of the centrifugal Rayleigh instability and its tendency to generate pairs of counterrotating vortex rings, as seen in the vorticity contours at $t = 0.801$ (Fig. 4b). The explanation lies in the fact that the swirl generates a strong radial gradient of the azimuthal velocity component. As a result, the azimuthal velocity component of a vortex line varies strongly along its arclength. Thus, there are segments of a vortex line that travel around the jet's axis at a higher angular velocity than neighboring segments of the same vortex line. Since the overall dynamics is inviscid, the vortex line has to stay connected, so that it necessarily has to fold back and forth, thereby generating azimuthal vorticity components of both signs. With increasing time, the emerging counterrotating ring becomes stronger (Fig. 5, $t = 1.225$), until two distinct counterrotating rings of opposite sign have emerged.

It should be pointed out that the circulation of each of the counterrotating rings, i.e., the integral over the positive (negative) azimuthal vorticity within one streamwise wavelength in the cross-cut, is a function of time, as the vortex filaments continue to wrap around the jet axis due to the differential azimuthal velocities experienced by different segments of the same vortex line. However, the sum of the circulations of two neighboring vortex rings of opposite sign remains constant with time. It is equal to the integral over one streamwise wavelength of the unperturbed initial azimuthal vorticity. In other words, while the circulations of the *individual* vortex rings grow indefinitely as a function of time, the sum of the circulation of a *pair of counterrotating vortices* does not depend on time. This is in contrast to the nonswirling configuration, where the circulation of individual vortex rings is independent of time.

In order to identify the formation, location, and size of any recirculation regions, it is of interest to analyze the bifurcation sequence of the streamline pattern, as seen in a reference frame moving with the velocity of the evolving jet shear layer structures, i.e., half the velocity of the unperturbed jet (Fig. 6). After the initial perturbation has been imposed, the streamlines show the familiar shape of the well-known Kelvin cats eyes ($t = 0.039$, Fig. 6a). With the emergence of counterrotating azimuthal vorticity, this topology changes, and an "island" forms midway between the Kelvin-Helmholtz vortices ($t = 0.625$, Fig. 6b). This island grows with time ($t = 1.016$, Fig. 6c), until it extends all the way to the jet centerline. Subsequently, a finite region of upstream velocity on the jet axis forms ($t = 1.436$, Fig. 6d), indicating the existence of a closed recirculation bubble. The different streamline pattern topologies are sketched in Figure 7.

The time-dependent evolution of the streamline pattern described above aids in the understanding of the transport of fluid towards and away from the jet axis. Between the counterrotating vortex rings, alternating regions exist in which the fluid velocity is directed towards larger and smaller radii, respectively. In this way, a certain 'pinch-off' effect is created, i.e., locally the jet diameter decreases dramatically.

Figure 8 shows the instantaneous growth rate of the circulation of the counterrotating vortex ring as a function of time, for different values of the dimensionless ratio $\Delta U_\theta / \Delta U_x$. Increased values of this parameter result in more rapid circulation growth, due to the increased role of the centrifugal instability. The figure demonstrates that, as a result of the inviscid nature of the present vortex dynamics calculations, the vortex ring circulation does not saturate.

The ways in which the Kelvin-Helmholtz instability interacts with the centrifugal instability, and how that interaction affects the strengthening of the counterrotating vortex ring, is illuminated by the following scaling argument. The azimuthal velocity of a jet shear layer vortex line segment can be approximated by the azimuthal velocity induced at its location by the centerline vortex, and by the streamwise vorticity contained in the layer itself. In this way, we obtain for the azimuthal velocity $v_{\theta 1}$ of the widest shear layer cross section, located at radius R_1 (Fig. 9)

$$v_{\theta 1} \approx \frac{\Gamma_c}{4\pi R_1} \tag{3}$$

where Γ_c is the circulation of the centerline vortex. A corresponding expression follows for the azimuthal velocity $v_{\theta 2}$ of the narrowest shear layer cross section, located at radius R_2. The above shows that different segments of the jet shear layer will rotate around the jet axis at different rotation rates. However, if a segment of the jet shear layer rotates at a different rate from a neighboring segment, the shear layer vorticity becomes increasingly reoriented into the azimuthal direction, thereby forming a vortex ring. The strength of this evolving vortex ring depends on the accumulated difference in the rotation between the neighboring segments. In particular, if one segment of a vortex line has rotated around the jet axis one more time than a nearby segment, a vortex ring has formed that has the circulation of the entire jet shear layer. Since this strength of the jet shear layer is equal and opposite to that of the centerline vortex, we have

$$2\pi R_0 \Delta U_\theta = -\Gamma_c \tag{4}$$

It follows immediately that the strength of the primary vortex ring, Γ_2, increases at the same rate as that of the secondary, counterrotating vortex, Γ_1, namely by the amount $\mid \Gamma_c \mid$ during the time interval ΔT that it takes for the narrowest cross section to complete one more rotation than the widest cross section. We obtain

$$\frac{d \mid \Gamma_1 \mid}{dt} = \frac{d \mid \Gamma_2 \mid}{dt} \approx \frac{\Gamma_c}{\Delta T} \tag{5}$$

With the above estimates for the azimuthal velocities of the cross sections, we then get the following estimates for the rate at which the circulation of the vortices increases

$$\frac{d \mid \Gamma_1 \mid}{dt} = \frac{\Gamma_c^2}{8\pi^2} \cdot \frac{R_1^2 - R_2^2}{R_1^2 R_2^2} \tag{6}$$

The temporal evolution of R_1 and R_2, in turn, depends on the growth of *both* the Kelvin-Helmholtz and the centrifugal instabilities. This point clearly demonstrates the nonlinear interaction between the two instability modes. The above scaling law relationship is shown in Figure 8, along with the computational results. For short times, the counterrotating ring has not yet formed, so that the above arguments do not yet apply. For long times, however, the agreement is quite good, considering the rough estimates on which the scaling law is based. It should be mentioned that, in the absence of viscous effects, the circulation of the counterrotating rings will grow without bounds, as a result of the continued interaction of the shear and centrifugal instabilities.

3.2 The Effect of Azimuthal Perturbations

The axisymmetric nature of the above calculation permits the evolution of concentrated vortical structures only in ring-like form. However, it is well known that three-dimensional perturbations to nominally two-dimensional[30,31,37,38] or axisymmetric[28,29] shear flows give rise to concentrated streamwise vortical structures that are predominantly located in the braid region. In order to investigate possible mechanisms for the generation of such structures in swirling jets, we introduce an azimuthal perturbation in addition to the axisymmetric one described above. Just like the axisymmetric perturbation, the azimuthal disturbance displaces the vortex filament centerline radially from its nominal location. Before the axisymmetric perturbation is applied, the distance r of a filament centerline is specified as a function of the circumferential coordinate ϕ by

$$r = R\left(1 + \epsilon_2 \cos\left(5\phi\right)\right) \tag{7}$$

in which ϵ_2 is the azimuthal disturbance amplitude. In an experiment, this type of perturbation can be imposed, for example, by means of a corrugated nozzle.[39] Due to the nonlinearity of the overall problem, the initial perturbation amplitude ratio represents an important parameter of the problem, as it can favor the rapid growth of one instability over others in their mutual competition. In particular, the early growth of one instability can affect the base flow in such a way as to suppress or accelerate the development of others. It should be pointed out that for this fully three-dimensional case, a Kelvin-Helmholtz instability of the streamwise vorticity can develop, in addition to the Kelvin-Helmholtz instability of the azimuthal vorticity and the centrifugal instability of the streamwise vorticity.

In the first one of the fully three-dimensional simulations, the ratio of the azimuthal and axial velocity jumps across the jet shear layer has the same value $\Delta U_\theta / \Delta U_x = 8.2$ as in the previous axisymmetric calculation. The azimuthal disturbance amplitude is relatively small at $\epsilon_2 = 0.04\%$, while the axisymmetric perturbation amplitude ϵ_1 is held constant at the level of five per cent (the same as above). The wavenumber of the azimuthal perturbation is taken to be five. As can be seen from Figure 10, the flow again develops two counterrotating vortex rings, as it did for the purely axisymmetric case. However, already the side view at $t = 0.977$ shows a slight nonuniformity in the azimuthal direction. By $t = 1.187$, concentrated streamwise braid structures have begun to form, as a result of a Kelvin-Helmholtz instability of the streamwise braid vorticity. It is interesting to note that these

braid vortices form only in the braid section *upstream* of the primary rings, i.e., in the narrow part of the braid. In contrast, the widening half of the braid region downstream of the primary rings does not exhibit any signs of concentrated streamwise vortical structures. The explanation for this behavior can be found in the effective wavelength change of the azimuthal Kelvin-Helmholtz instability due to the radial velocity component. In those regions where the braid circumference grows, the growth of the Kelvin-Helmholtz instability in the circumferential direction is slowed down as its effective wavelength increases, whereas in the narrowing braid sections the instability is accelerated due to the wavelength reduction.

It is important to point out that the streamwise vortex structures are all of the same sign, i.e., they are *corotating*. The reason for this lies in the fact that the braid vorticity, which forms the streamwise structures by a process of concentration as a result of a Kelvin-Helmholtz instability, is of the same sign everywhere. In this aspect, the evolution of the braid region resembles the situation encountered in a nonswirling jet disturbed by a helical and an azimuthal wave.[29] In contrast to the counterrotating vortex rings, the circulation of the streamwise braid vortices cannot grow without bounds. Rather, it is limited by the fact that, within a $x = const.$ cross section of the jet, the circulation of the jet shear layer vorticity has to be equal and opposite to that of the centerline vortex. Consequently, the maximum strength of the streamwise braid vortices, achieved if all the jet shear layer vorticity is contained in these concentrated structures, is equal to the circulation of the centerline vortex divided by the azimuthal wavenumber.

The above observations are confirmed by the isosurface plot of the vorticity magnitude in Figure 11 for $t = 1.343$. It shows the counterrotating vortex rings, connected in one half of the braid region by concentrated streamwise vortical structures. A tendency of the braid vortices to wrap around the vortex rings is visible as well.

Figure 12 shows the evolution of a flow if the azimuthal perturbation amplitude is increased to $\epsilon_2 = 1\%$, while the axisymmetric disturbance amplitude is left unchanged at $\epsilon_1 = 5\%$. This increase in the perturbation amplitude ratio is expected to lead to an increased growth of the azimuthal Kelvin-Helmholtz instability, and consequently to a more rapid evolution of concentrated streamwise vortical structures. In addition, the ratio of the azimuthal and axial velocity jumps across the jet shear layer is reduced to $\Delta U_\theta / \Delta U_x = 3.0$. In this way, the development of the centrifugal instability, and with it the formation of the counterrotating ring, is slowed down. As a result, at time 2.402 we recognize concentrated primary vortex rings, connected by strong streamwise braid vortices that now extend over the *entire* length of the braid region. This early formation of streamwise vortices has preempted any coherent directional reversal of the vortex filament portions, so that counterrotating vortex rings have not formed in this flow. However, the centrifugal instability still causes the braid vortices themselves to acquire a strong azimuthal component, thereby generating a staggered pattern, as can be seen at $t = 3.154$. This is confirmed by the three-dimensional isosurface plot, which shows primary vortex rings connected by strong wavy streamwise braid vortices.

This evolution of the flow for $\epsilon_2 = 0.01$ is a typical result of the above mentioned competition between the various instability mechanisms. Under these conditions, the growth

of the Kelvin-Helmholtz instability of the streamwise vorticity is accelerated compared to that of the centrifugal instability, so that nearly all of the braid vorticity between the primary vortex rings becomes concentrated in streamwise vortices before counterrotating rings can form.

Fig. 13 shows results for $\Delta U_\theta / \Delta U_x = 3.0$ and $\epsilon_2 = 0.05$, i.e., for an even higher azimuthal perturbation amplitude. As a result, the growth of the Kelvin-Helmholtz instability in the azimuthal direction is further amplified, so that now even the primary vortex rings develop only very weakly. Already at $t = 1.543$, strong and slightly wavy streamwise vortices have formed, and a weak tendency towards the formation of the primary rings is visible. At $t = 3.105$ we recognize that the wavy sections of the streamwise structures align themselves in such a way that, together, they nearly form a ring-like structure at the locations where primary rings should develop, although they remain disconnected. Consequently, the three-dimensional isosurface plot shows that for the present flow parameters the swirling jet is dominated by wavy streamwise structures, while neither primary nor secondary counterrotating vortex rings seem to play an important role.

In the literature on swirling flows, it is common to quantify the effect of swirl in terms of a swirl number S (e.g., Panda and McLaughlin[13]), and to then characterize the behavior of the flow as a function of this parameter. The usual definition of S is

$$S = \frac{\dot{G}_\theta}{R \dot{G}_x} \quad , \quad \dot{G}_\theta = 2\pi \int_0^\infty \rho U W r^2 dr \quad , \quad \dot{G}_x = 2\pi \int_0^\infty \left(\rho U^2 + p \right) r dr \tag{8}$$

which gives the ratio of the axial flux of tangential momentum $\dot{G}_\theta$ to the product of the radius R and the axial flux of axial momentum $\dot{G}_x$. For a vanishing jet shear layer thickness, the above integration over our unperturbed initial velocity profile can be carried out analytically. However, the result depends on the selected reference frame. When compared to the experimental situation of a swirling jet entering a large body of fluid at rest, the proper computational reference frame is the one in which the jet fluid has unit velocity in the streamwise direction, with the fluid outside the jet being at rest. We then obtain

$$S = \frac{\Gamma_c}{2\pi R} \tag{9}$$

However, it is clear from the above that this definition of the swirl number is not very meaningful in characterizing the effect of swirl in the present flow model, because it does not take into account the presence of streamwise vorticity in the axisymmetric shear layer, which is the cause for the centrifugal instability. Consequently, the usual definition of the swirl number cannot be employed in a meaningful way to distinguish different flow regimes for the present flow model.

4 Summary and Conclusions

The dynamical evolution of swirling jets is characterized by the complex nonlinear interaction of several different competing instability mechanisms. The axial, jet-like velocity profile

gives rise to a Kelvin-Helmholtz instability of the azimuthal vorticity component, thereby favoring the formation of like-signed vortex rings, as is well known from investigations of nonswirling jets. However, the additional azimuthal velocity component of the base flow introduces streamwise vorticity as well, whose existence allows for further instabilities to develop. Firstly, there is the possibility for a centrifugal instability to arise, which tends to promote the evolution of counterrotating vortex rings; i.e., rings of both the same as well as of opposite sign compared to those found in nonswirling jets. Secondly, if the streamwise vorticity is mainly concentrated in a narrow shear layer surrounding the jet axis, it can also be subject to a Kelvin-Helmholtz instability in the *azimuthal* direction, which can lead to the evolution of concentrated streamwise vortices.

In order to gain some insight into the nonlinear mechanisms of interaction and competition between these various potential instabilities, we performed nonlinear, inviscid, three-dimensional vortex dynamics simulations for a simplified model of swirling jets. The nature of the model is such that it allows for the easy identification of the various mechanisms at work. By tracking the nonlinear evolution of vortex lines, it enables us to investigate the effects of the centrifugal instability, as well as of the Kelvin-Helmholtz instabilities feeding on both the azimuthal and the streamwise vorticity, onto processes of concentration, reorientation, and stretching of vorticity. The drawback of the present model is that it does not have easily adjustable parameters allowing for the representation of the wide variety of experimentally generated, and often geometry dependent, base flow profiles. In particular, a study of the dynamics of very smooth, Gaussian-like streamwise and azimuthal velocity profiles will have to be based on the evolution of a more continuous initial vorticity distribution, rather than the shear layer model employed here. With this in mind, the current investigation has to be seen as a first step, intended to provide qualitative information on a variety of dynamical mechanisms and their interactions, and to be followed by three-dimensional Navier-Stokes or vortex particle simulations. Nevertheless, the present model elucidates many of the key features expected to dominate the evolution of swirling jets. In particular the formation of counterrotating vortex rings, whose strength increases with time as a result of the continued interaction between shear and centrifugal instabilities, seems to represent a general phenomenon that one would expect to observe in a viscous flow as well. The quantitative growth, however, and in particular the exact form of the scaling law given by eqn. (7) would certainly be a function of the prescribed initial streamwise and azimuthal velocity profiles. In the same way, the exact perturbation amplitudes resulting in more or less dominant streamwise vortical structures will vary with these profiles as well. Even for more general velocity profiles we do expect, however, to observe different flow regimes dominated by different large scale vortical structures, along the lines described above.

A main goal lies in the investigation of the mechanisms by which the introduction of swirl affects the dynamics observed earlier for nonswirling jets.[28,29] Conversely, the question arises as to how the purely swirling flow examined by Caflisch, Li, and Shelley[21] is modified by the addition of an axial velocity component. We find that the main effect of the added streamwise velocity lies in the breaking of the symmetry of the pure swirling flow. As a result, the counterrotating rings observed in the purely swirling flow are no longer of equal

strength, as one of them is amplified, and the other one weakened, by the Kelvin-Helmholtz instability of the axial flow. On the other hand, the introduction of swirl drastically alters the dynamics of nonswirling jets, as it results in the formation of counterrotating vortex rings, whose circulations, in the absence of viscous effects, can grow in time without bounds. These rings promote a pinch-off mechanism leading to a dramatic decrease in the local jet diameter.

While the above mechanisms can be observed in axisymmetric swirling jets, an additional azimuthal perturbation leads to the formation of concentrated streamwise vortices as a result of a Kelvin-Helmholtz instability feeding on the streamwise jet shear layer vorticity. In contrast to nonswirling jets, the streamwise vortices in swirling jets are all of the same sign. The nature of the large scale vortical structures dominating the long term dynamics of the jet depends strongly on the ratio of the initial perturbation amplitudes in the azimuthal and streamwise directions. If this ratio is small, the centrifugal instability has enough time to form counterrotating vortex rings, before concentrated streamwise vortices can emerge in the braid regions between them. For a somewhat larger perturbation amplitude ratio, streamwise vortices grow more rapidly in the braid region between the like-signed primary vortex rings. In this way, they suppress the growth of the counterrotating rings. However, the centrifugal effects lead to a partial reorientation of the braid vortices in the azimuthal direction. Finally, for even larger initial azimuthal perturbation amplitudes, the streamwise vortices grow fast enough to suppress the growth of even the primary corotating vortex rings. In this case, the long term dynamics of the swirling jet is dominated by wavy like-signed axial vortical structures.

The above description is predominantly qualitative, and a more detailed quantitative investigation of these effects is clearly necessary. In particular, it will be of interest to study the competition between the different instability mechanisms as a function of the detailed shape of the base flow profile. Furthermore, the effect of helical rather than axisymmetric perturbations, and their interaction with azimuthal disturbances, needs to be addressed. Eventually, investigations of simplified swirling jet models such as the present one are expected to provide some guidance for carrying out and interpreting three-dimensional spatially growing, fully viscous simulations of swirling jets. It is hoped that an investigation along those lines might also help to shed some light onto the various forms of vortex breakdown observed in swirling jets.

References

[1] Gupta, A.K., Lilley, D.G. and Syred, N. *Swirl Flows*, Kent, Engl: Abacus (1984).

[2] Escudier, M. "Confined vortices in flow machinery," Ann. Rev. Fluid Mech. **19**, 27 (1987).

[3] Wygnanski, I. "Swirling axisymmetrical laminar jet," Phys. Fluids **13**, 2455 (1970).

[4] Burggraf, O.R. and Foster, M.R. "Continuation or breakdown in tornado-like vortices," J. Fluid Mech. **80**, 645 (1977).

[5] Stewartson, K. "The stability of swirling flows at large wavenumber when subjected to disturbances with large azimuthal wavenumber," Phys. Fluids **25**, 1953 (1982).

[6] Leibovich, S. and Stewartson, K. "A sufficient condition for the instability of columnar vortices," J. Fluid Mech. **126**, 335 (1983).

[7] Toplosky, N. and Akylas, T.R. "Nonlinear spiral waves in rotating pipe flow," J. Fluid Mech. **190**, 39 (1988).

[8] Foster, M.R. "Nonaxisymmetric instability in slowly swirling jet flows," Phys. Fluids A **5**, 3122 (1993).

[9] Chigier, N.A. and Chervinsky, A. "Experimental investigation of swirling vortex motion in jets," Trans. ASME, J. Appl. Mech. **34**, 443 (1967).

[10] Farokhi, S., Taghavi, R. and Rice, E.J. "Effect of initial swirl distribution on the evolution of a turbulent jet," AIAA J. **27**, 700 (1989).

[11] Frey, M.O. and Gessner, F.B. "Experimental investigation of coannular jet flow with swirl along a centerbody," AIAA J. **29**, 2132 (1991).

[12] Mehta, R.D., Wood, D.H. and Clausen, P.D. "Some effects of swirl on turbulent mixing layer development," Phys. Fluids A **3**, p. 2716 (1991).

[13] Panda, J. and McLaughlin, D.K. "Experiments on the instabilities of a swirling jet," Phys. Fluids A **6**, 263 (1994).

[14] Lopez, J.M. "Axisymmetric vortex breakdown. Part 1: Confined swirling flow," J. Fluid Mech. **221**, 533 (1990).

[15] Brown G.L. and Lopez, J.M. "Axisymmetric vortex breakdown. Part 2: Physical mechanism," J. Fluid Mech. **221**, 553 (1990).

[16] Lopez, J.M. and Perry, A.D. "Axisymmetric vortex breakdown. Part 3: Onset of periodic flow and chaotic advection," J. Fluid Mech. **234**, 449 (1991).

[17] Althaus, W., Brucker, C., and Weimer, M. "Breakdown of slender vortices," in: *Fluid Vortices*, ed. S.I. Green, Kluwer (1995).

[18] Martin, J.E. and Meiburg, E. "On the stability of the swirling jet shear layer," Phys. Fluids A **6**, 424 (1994).

[19] Batchelor, G.K. and Gill, A.E. "Analysis of the stability of axisymmetric jets," J. Fluid Mech. **14**, 529 (1962).

[20] Rotunno, R. "A note on the stability of a cylindrical vortex sheet," J. Fluid Mech. **87**, 761 (1978).

[21] Caflisch, R.E., Li, X., and Shelley, M.J. "The collapse of an axi-symmetric swirling vortex sheet," Nonlinearity **6**, 843 (1993).

[22] Martin, J.E. and Meiburg, E. "The nonlinear evolution of swirling jets," Meccanica **29**, 331 (1994).

[23] Shariff, K. and Leonard, A. "Vortex rings," Ann. Rev. Fluid Mech. **24**, 235 (1992).

[24] Moffatt, H.K. "Generalized vortex rings with and without swirl," Fl. Dyn. Res. **3**, 22 (1988).

[25] Turkington, B. "Vortex rings with swirl: Axisymmetric solutions of the Euler equations with nonzero helicity," SIAM J. Math. Anal. **20**, 57 (1989).

[26] Lifschitz, A. and Hameiri, E. "Localized instabilities of vortex rings with swirl," Comm. Pure Appl. Math. **46**, 1379 (1993).

[27] Virk, D., Melander, M.V. and Hussain, F. "Dynamics of a polarized vortex ring," preprint (1993).

[28] Martin, J.E. and Meiburg, E. "Numerical investigation of three-dimensionally evolving jets subject to axisymmetric and azimuthal perturbations," J. Fluid Mech. **230**, 271 (1991).

[29] Martin, J.E. and Meiburg, E. "Numerical investigation of three-dimensionally evolving jets under helical perturbations," J. Fluid Mech. **243**, 457 (1992).

[30] Ashurst, W.T. and Meiburg, E. "Three-dimensional shear layers via vortex dynamics," J. Fluid Mech. **189**, 87 (1988).

[31] Meiburg, E. and Lasheras, J.C. "Experimental and numerical investigation of the three-dimensional transition in plane wakes," J. Fluid Mech. **190**, 1 (1988).

[32] Lasheras, J.C. and Meiburg, E. "Three-dimensional vorticity modes in the wake of a flat plate," Phys. Fluids A **2**, 371 (1990).

[33] Leonard, A. "Computing three-dimensional flows with vortex elements," Ann. Rev. Fluid Mech. **17**, 523 (1985).

[34] Meiburg, E. "Three-dimensional vortex dynamics simulations," in: *Fluid Vortices*, ed. S.I. Green, Kluwer (1995).

[35] Michalke, A. and Hermann, G. "On the inviscid instability of a circular jet with external flow," J. Fluid Mech. **114**, 343 (1982).

[36] Gaster, M. "A note on the relation between temporally-increasing and spatially-increasing disturbances in hydrodynamic stability," J. Fluid Mech. **14**, 222 (1962).

[37] Bernal, L.P. and Roshko, A. "Streamwise vortex structures in plane mixing layers," J. Fluid Mech. **170**, 499 (1986).

[38] Lasheras, J.C. and Choi, H. "Three-dimensional instability of a plane, free shear layer: an experimental study of the formation and evolution of streamwise vortices," J. Fluid Mech. **189**, 53 (1988).

[39] Martin, J.E., Meiburg, E., and Lasheras, J.C. "Three-Dimensional Evolution of Axisymmetric Jets: A Comparison between Computations and Experiments,"in: *Separated Flows and Jets*, eds. V.V. Kozlov and A.V. Dovgal, Springer Verlag, Berlin (1991).

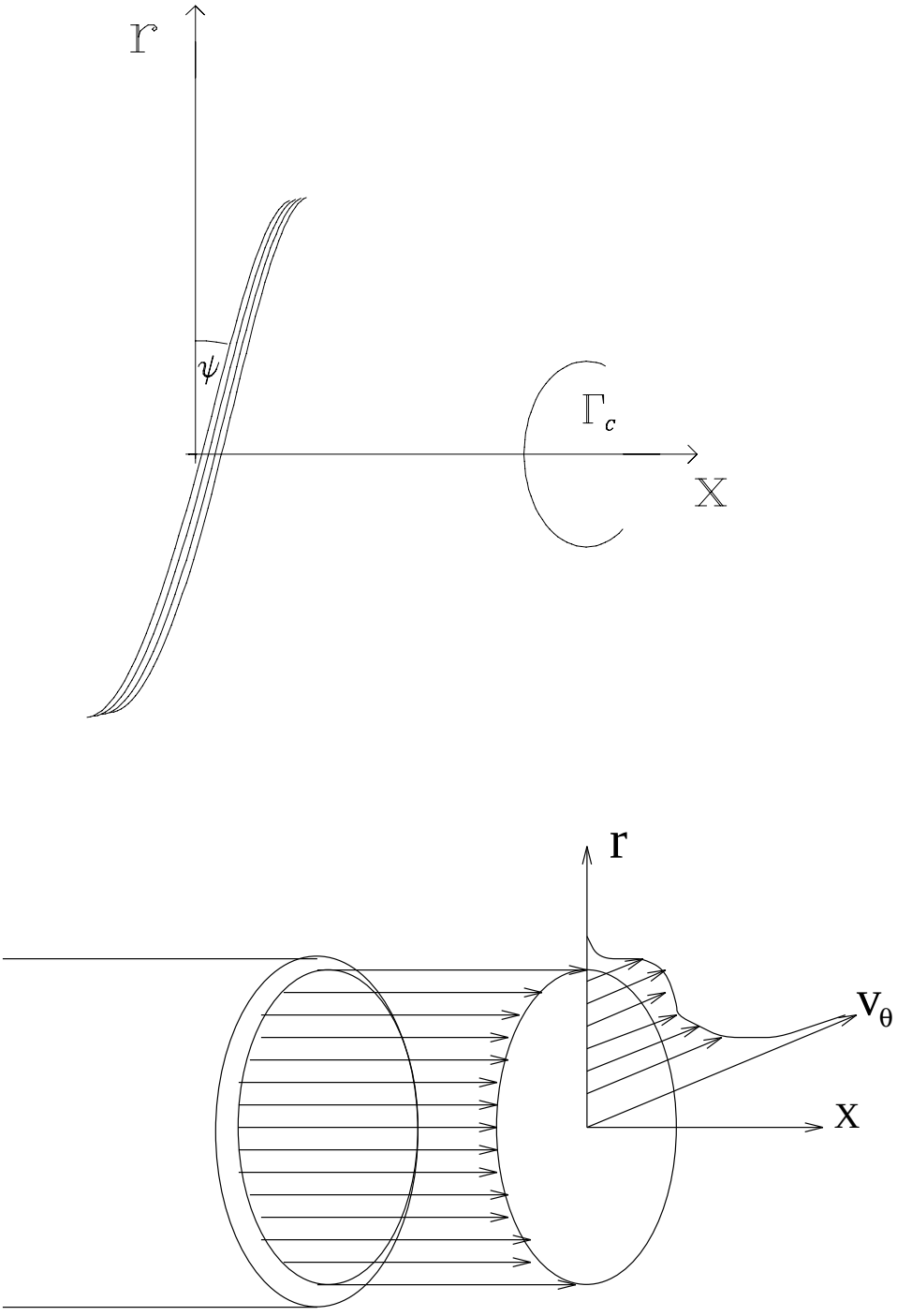

Figure 1: Simplified model of a swirling jet flow. The centerline vortex of strength Γ_c is surrounded by a nominally axisymmetric jet shear layer containing helical vortex lines of pitch ψ. The azimuthal vorticity component is related to the top hat axial velocity profile, whereas the streamwise vorticity component results in the centrifugally unstable stratification. Also shown are the streamwise and azimuthal base flow velocity profiles.

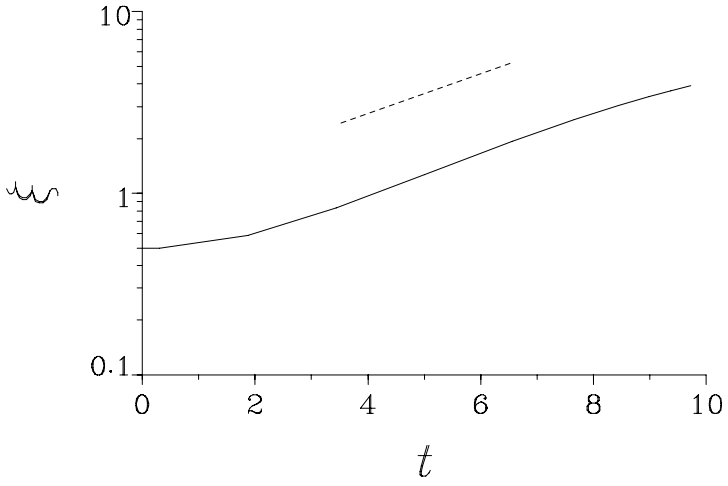

Figure 2: Comparison of the numerical growth rates of the radial perturbation amplitude obtained from the vortex filament simulation (solid line) and the analytical growth rate (dotted line) for the case of a purely swirling flow.

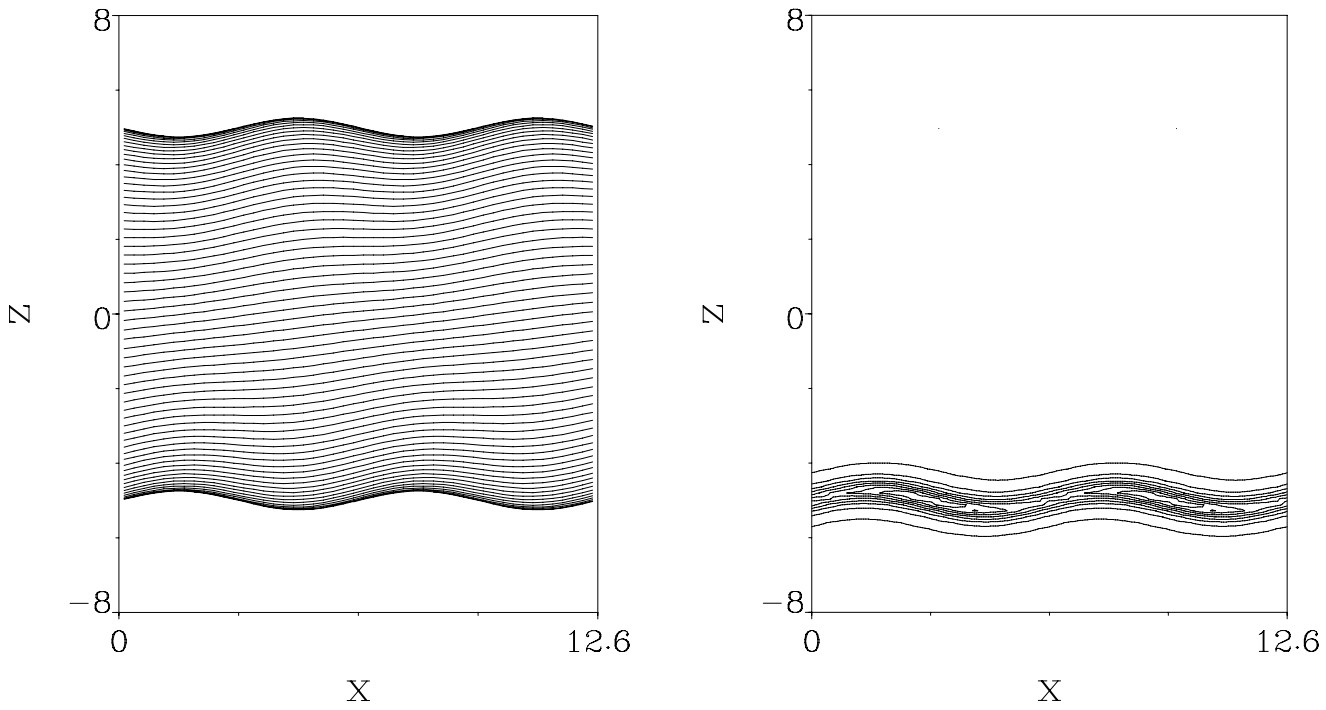

Figure 3: The evolution of a swirling jet with $\Delta U_\theta / \Delta U_x = 8.2$ subject to an axisymmetric perturbation. Shown is a side view of the vortex filaments at time $t = 0.039$ (a), along with isocontours of the azimuthal vorticity distribution in a cross section containing the jet axis (b). For clarity, two streamwise wavelengths are shown. Initially, the vortex lines are predominantly oriented in the streamwise direction. At this early time, both graphs indicate that the azimuthal vorticity component points in the same direction everywhere in the vortex sheet. This is a reflection of the early stages of corotating ring formation due to the Kelvin-Helmholtz instability of the azimuthal vorticity component.

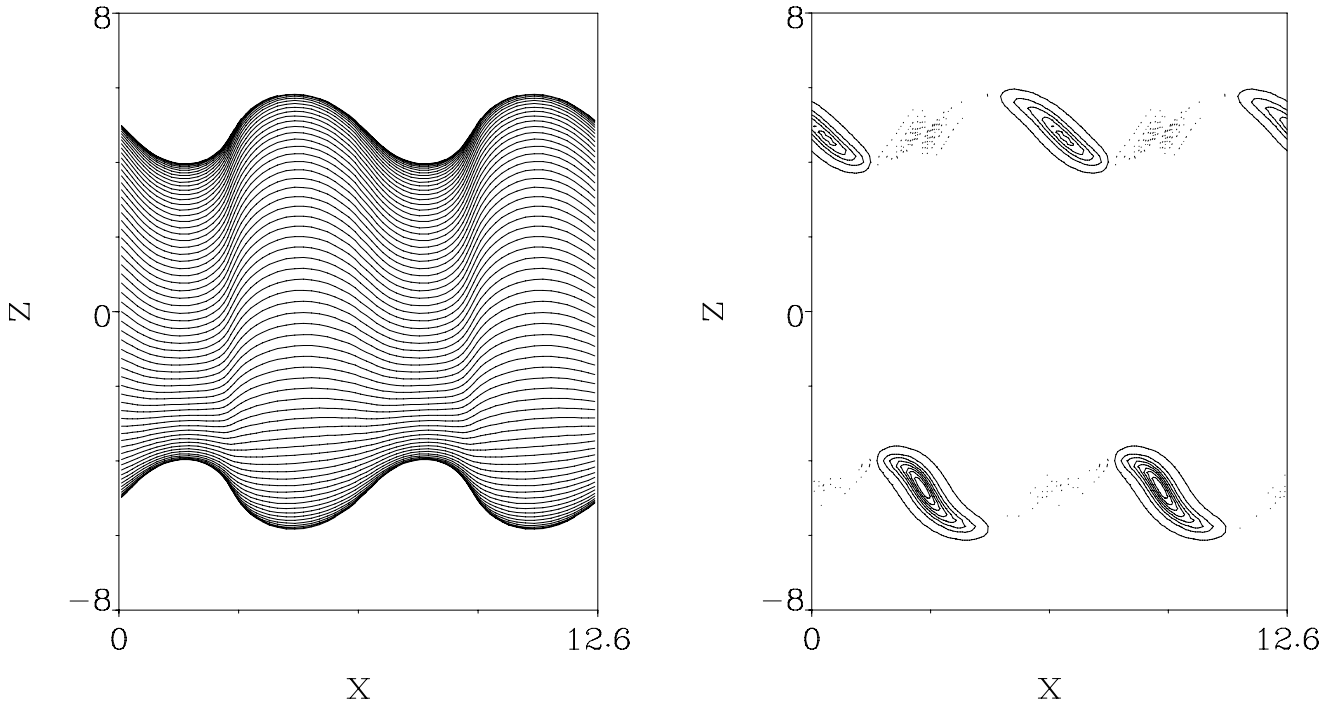

Figure 4: Time 0.801: Counterrotating rings form in the braid regions between the primary vortices, as a result of a centrifugal instability related to the streamwise vorticity. The rings form as a result of the reorientation of certain vortex filament segments into the opposite azimuthal direction near $x = 0$ and $x = 2\pi$, respectively.

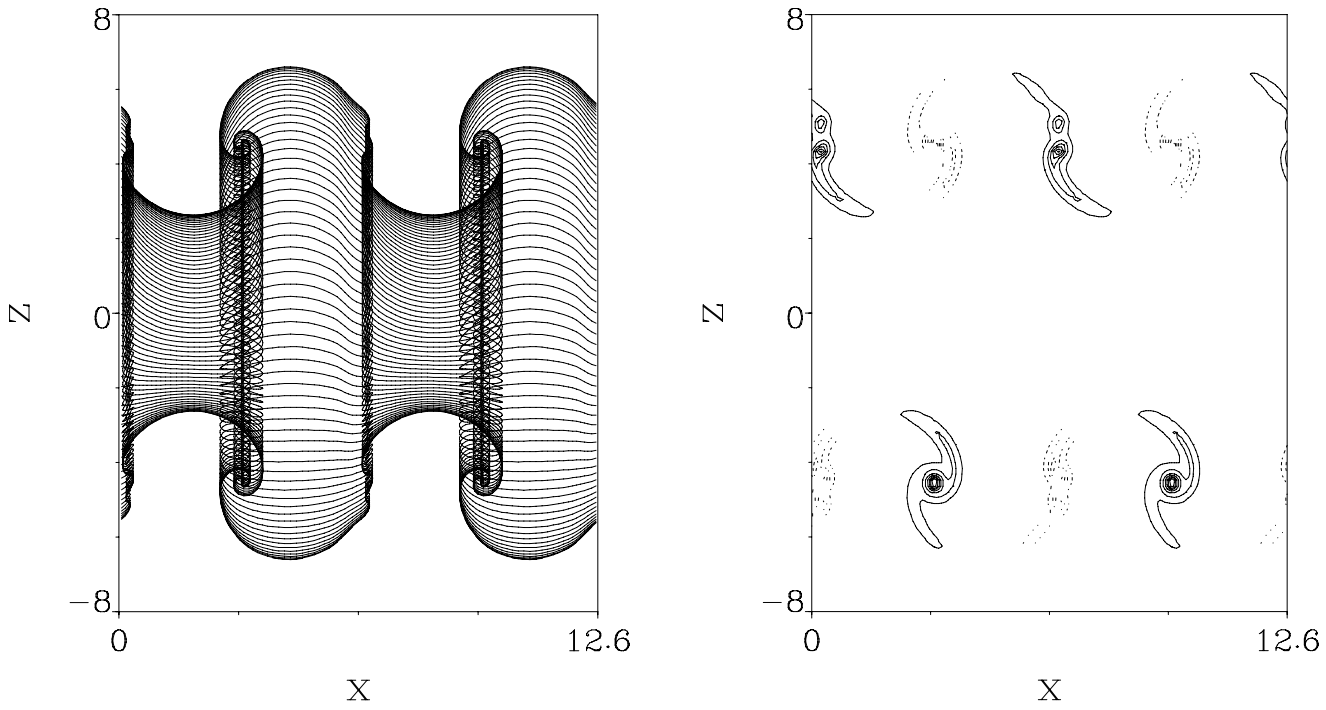

Figure 5: Time 1.225: The counterrotating rings increase in strength, leading to the formation of alternating regions in which fluid is convected towards or away from the jet axis, respectively.

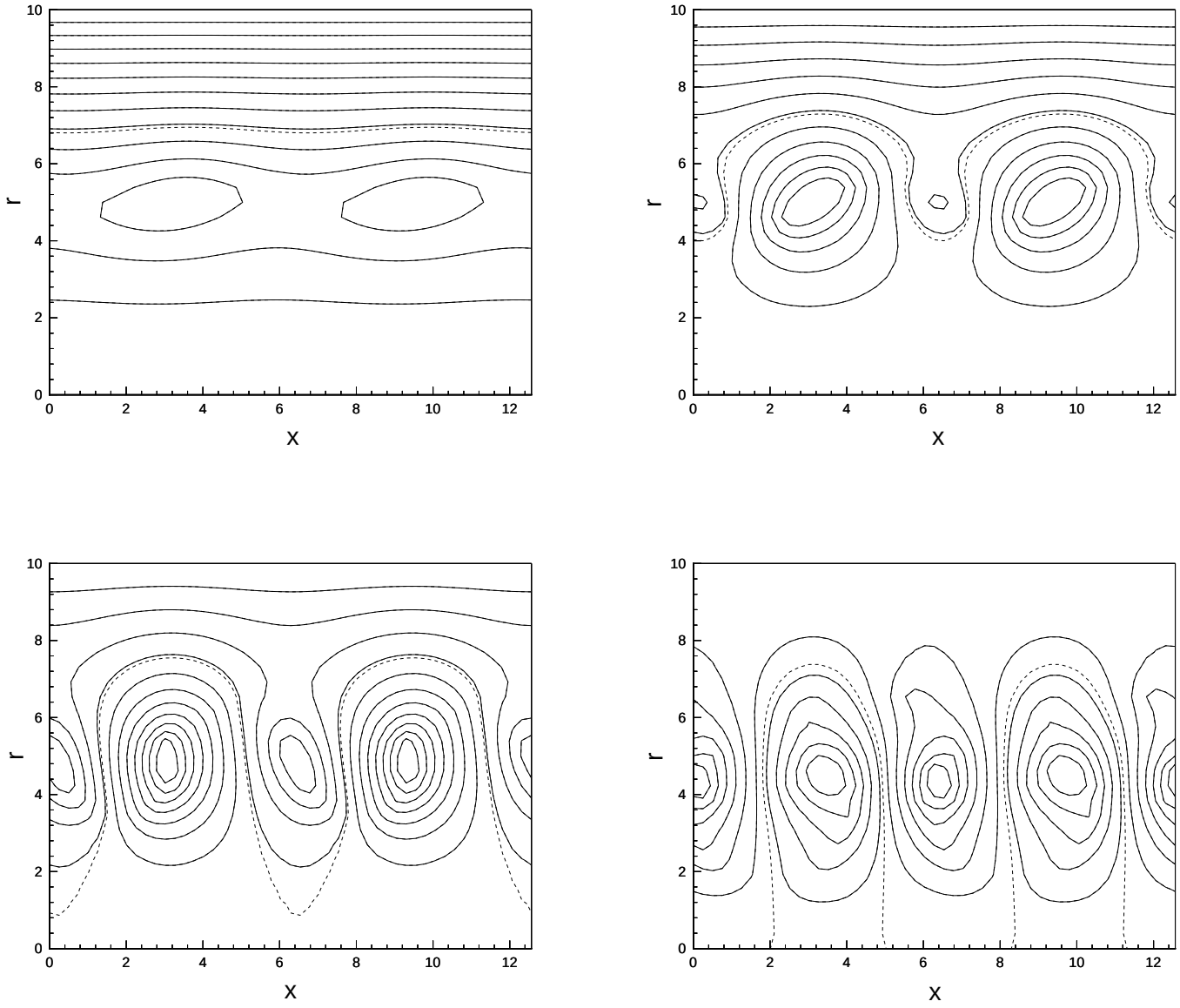

Figure 6: The sequence of bifurcations of the streamline pattern as seen in the reference frame moving with half the nominal jet velocity. Islands form in the initial cats eyes pattern. Subsequently, these islands grow in size, until they extend to the jet axis, where they create regions of upstream velocity. In all frames, the dotted contour line has the same value as the jet centerline.

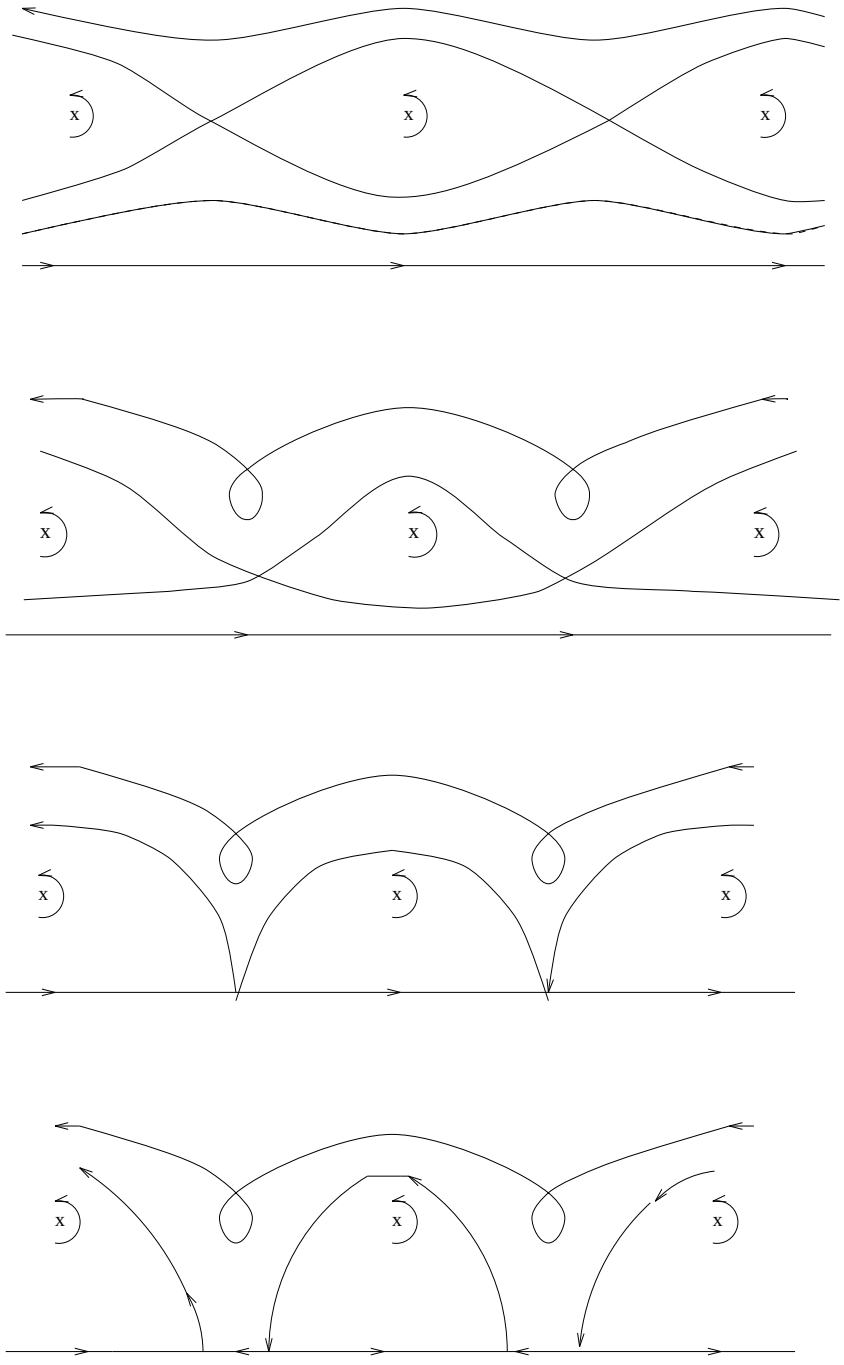

Figure 7: Sketch of the sequence of different streamline pattern topologies.

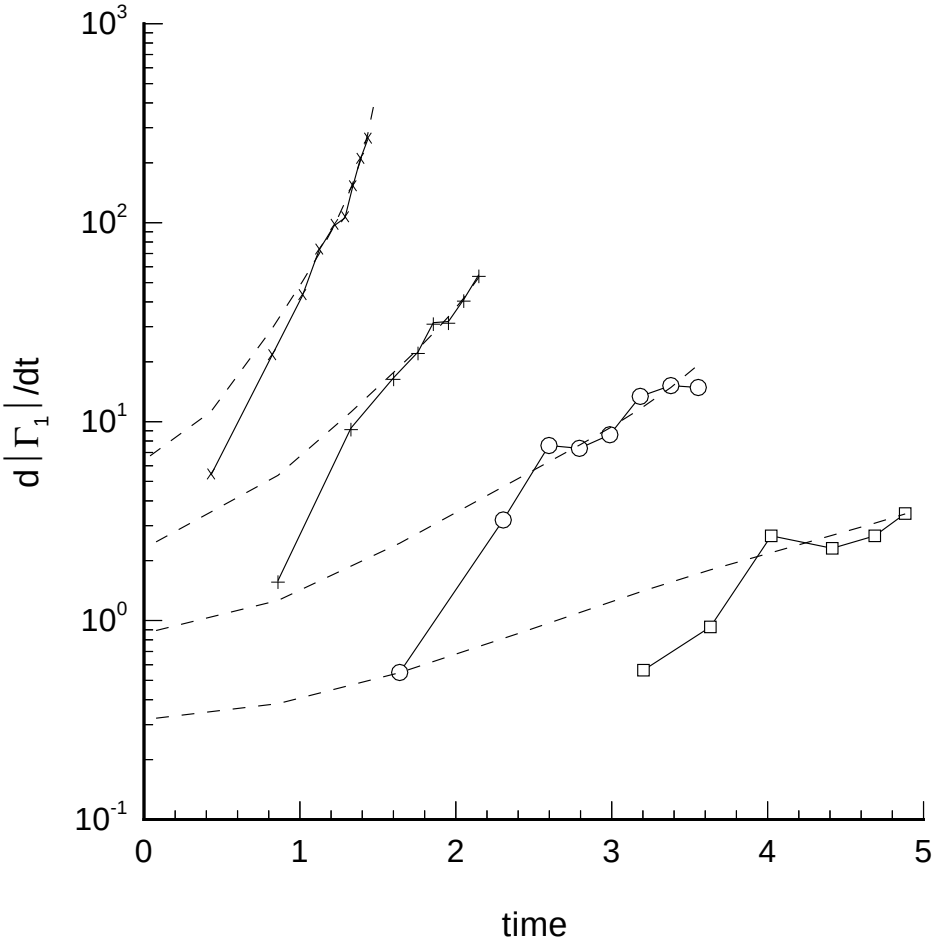

Figure 8: Instantaneous growth rate of the circulation of the counterrotating vortex ring as a function of time. The dimensionless ratio $\Delta U_\theta / \Delta U_x$ has the following values: x:8.2, +:5.0, o:3.0, □:1.8. Also plotted are the corresponding time-dependent values obtained from the scaling law (dashed lines). For longer times, the agreement between the scaling law expressions and the numerical values improves.

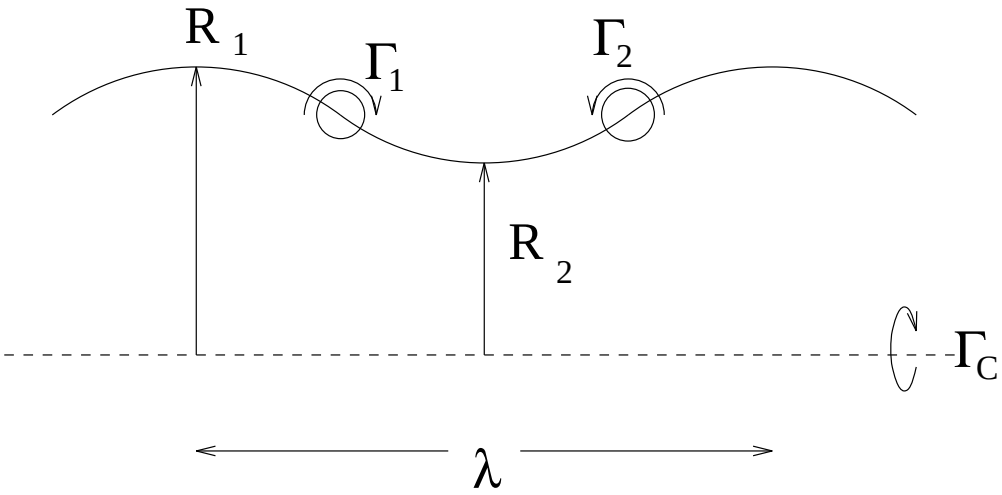

Figure 9: Definitions of quantities used in the scaling arguments.

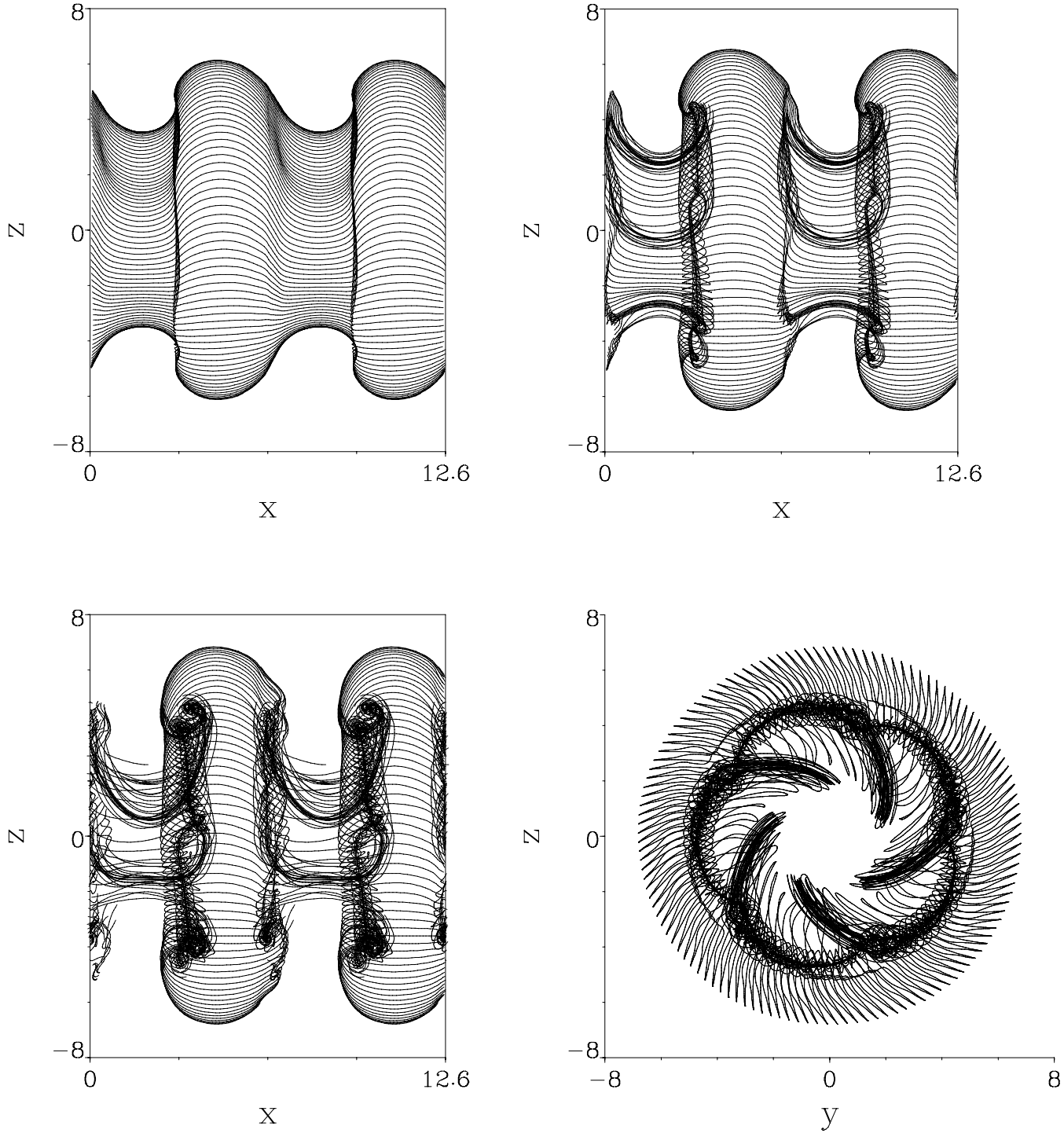

Figure 10: Evolution of a swirling jet with $\Delta U_\theta/\Delta U_x = 8.2$ subject to an axisymmetric perturbation of amplitude 5%, and an azimuthal disturbance of amplitude 0.04%. Shown are side views at times 0.977, 1.187, and 1.343, along with an end view for $t = 1.343$. The formation of the primary and counterrotating rings proceeds similarly to the axisymmetric case displayed in Figures 3 to 5. However, the azimuthal disturbance leads to the formation of additional concentrated streamwise vortical structures in the narrow half of the braid region.

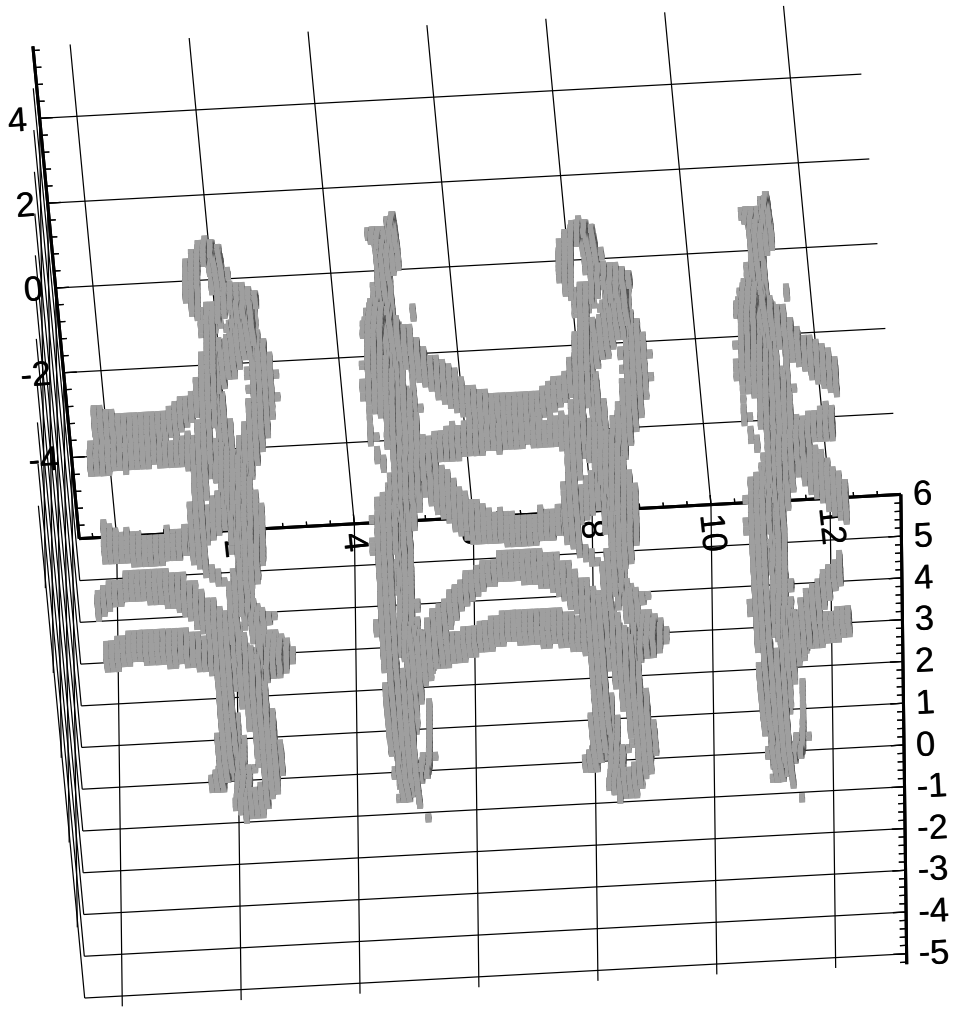

Figure 11: Isosurface plot of the vorticity magnitude for the flow shown in Figure 10 at $t = 1.343$. The dominant large scale coherent vortical structures have the form of primary and secondary vortex rings, with additional streamwise vortices located in the narrow section of the braid region.

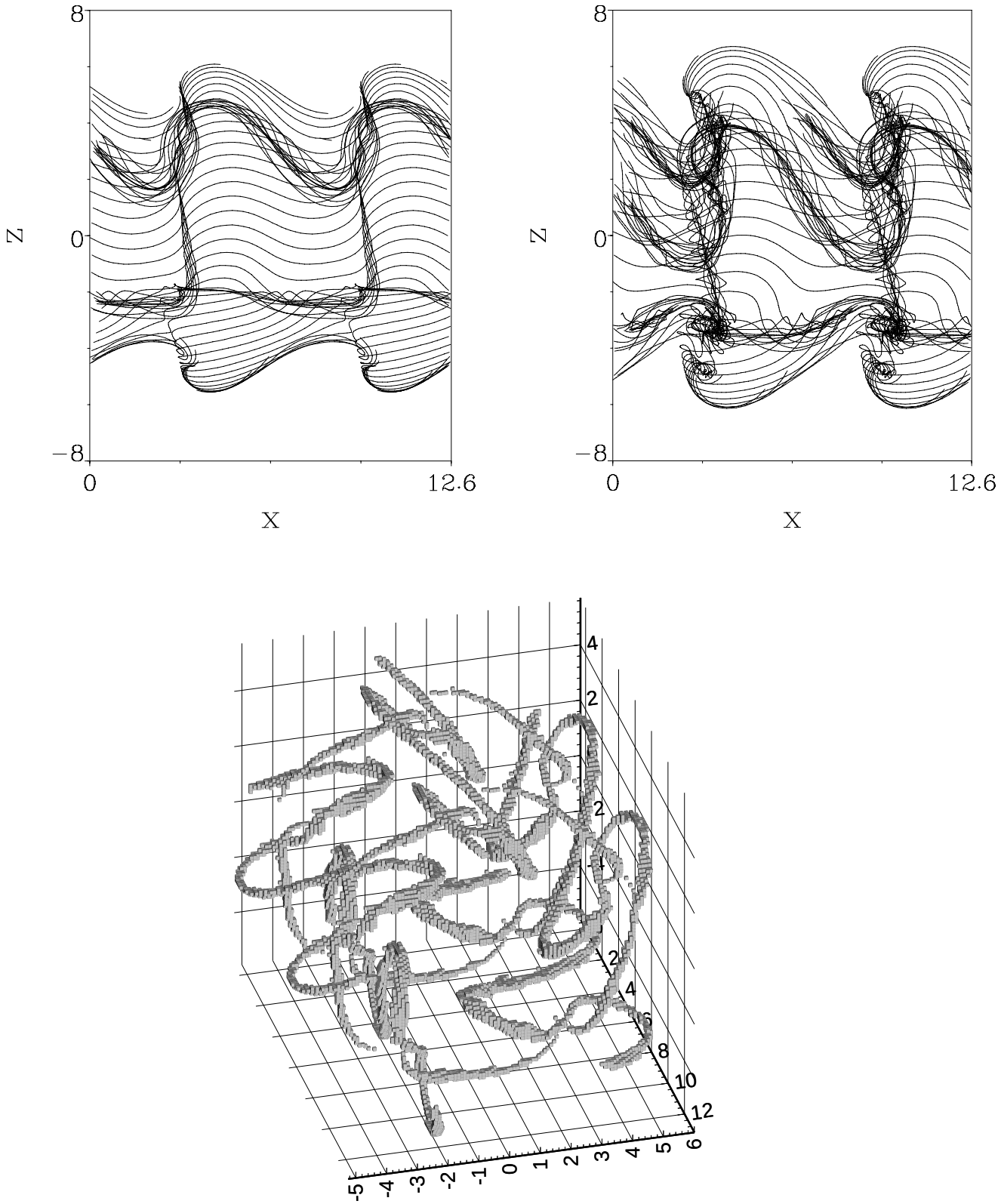

Figure 12: Evolution of a swirling jet with $\Delta U_\theta/\Delta U_x = 3$ subject to an axisymmetric perturbation of amplitude 5%, and an azimuthal disturbance of amplitude 1%. Shown are side views at times 2.402 and 3.154, along with a vorticity magnitude isosurface plot for this later time. For these parameters, the streamwise vortical structures develop more rapidly, and they prevent the formation of the secondary counterrotating vortex rings. The isosurface plot shows the dominant large scale structures to have the form of distorted vortex rings, connected by wavy streamwise vortical structures.

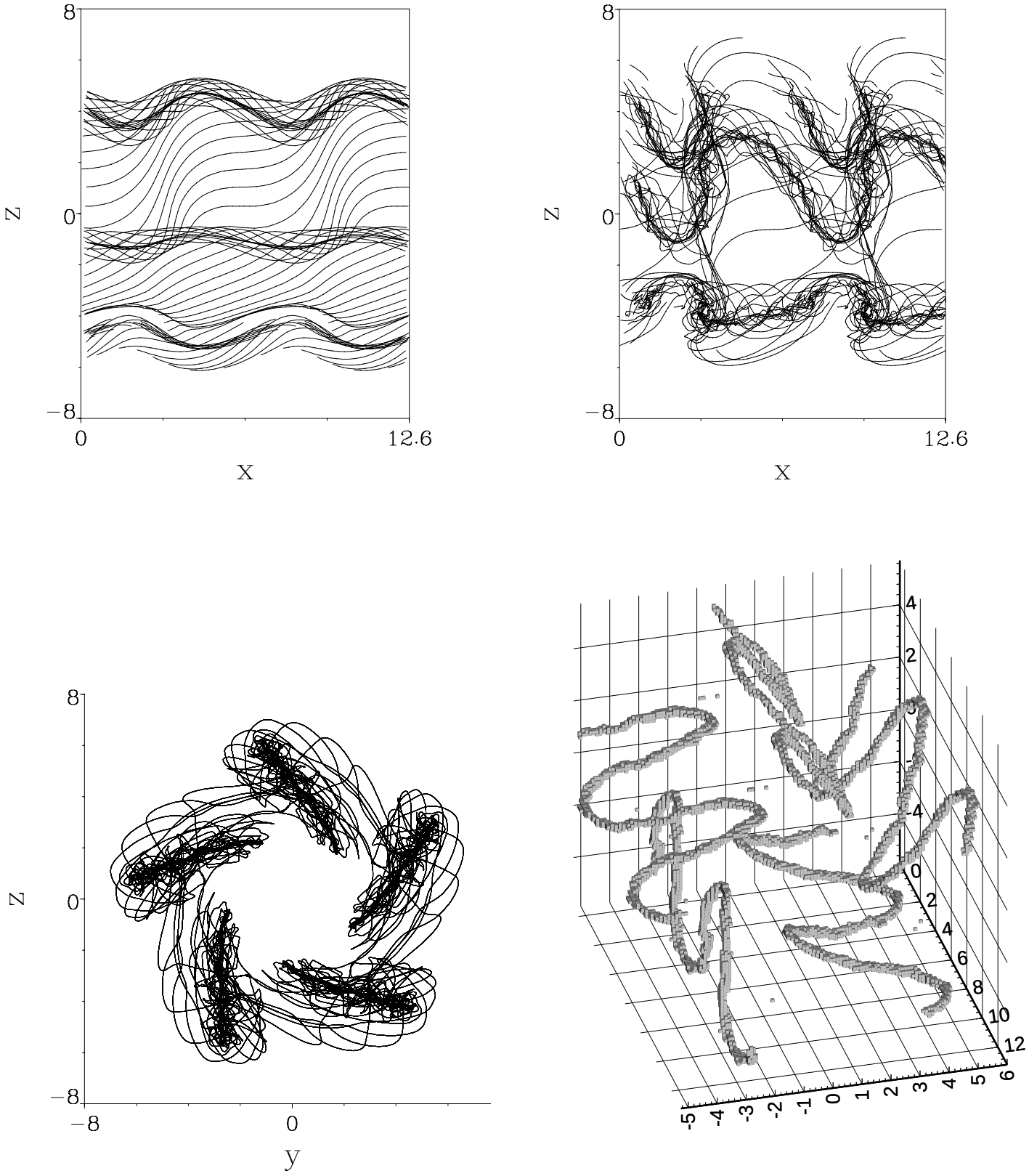

Figure 13: Evolution of a swirling jet with $\Delta U_\theta/\Delta U_x = 3$ subject to an axisymmetric perturbation of amplitude 5%, and an azimuthal disturbance of amplitude 5%. Shown are side views at times 1.543 and 3.105, along with an end view and a vorticity magnitude isosurface plot for this later time. Here, the streamwise vortical structures develop even more rapidly, thereby suppressing even the formation of strong primary vortex rings. Consequently, the isosurface plot shows wavy streamwise vortices to dominate the large scale features of the flow.